IEEE Access
Multidisciplinary | Rapid Review | Open Access Journal

Received August 25, 2019, accepted September 20, 2019, date of publication September 25, 2019, date of current version October 8, 2019.

Digital Object Identifier 10.1109/ACCESS.2019.2943775

Analysis of Temperature Field and Water Cooling of Outer Rotor In-Wheel Motor for Electric Vehicle

QIPING CHEN, HAO SHAO, JUANLIN HUANG, HAOYU SUN, AND JIACHAO XIE
Key Laboratory of Conveyance and Equipment of the Ministry of Education, East China Jiaotong University, Nanchang 330013, China

Corresponding author: Qiping Chen (qiping3846758@163.com)

This work was supported in part by the National Natural Science Foundation of China under Grant 51565011, in part by the Natural Science Foundation for Distinguished Young Scholars of Jiangxi Province under Grant 20171BCB23059, in part by the Key Research Program of Jiangxi Province under Grant 20171BBE50039, and in part by the Natural Science Foundation of Jiangxi Province under Grant 20171BAB216027.

ABSTRACT In view of the narrow installation space of high power density and high torque in-wheel motor, the heat existed the in-wheel motor is balanced by cooling water channel to ensure the heat dissipation of the high power density in-wheel motor. In this paper, Ansoft Maxwell software is used to establish the two-dimensional loss simulation model of in-wheel motor, and the winding loss, stator core loss, rotor core loss and permanent magnet eddy current loss of in-wheel motor are calculated respectively. The temperature field calculation model of in-wheel motor is established. The heat exchange coefficient of motor is calculated, and the equivalent treatment of windings is carried out. The spiral channel is selected to cool the motor. The CFD software is used to simulate and analyze the cooling fluid in the channel. The heat dissipation coefficient curve is calculated. Finally, the calculated results of in-wheel motor loss and heat dissipation coefficient curve are imported into the transient temperature field for simulation, and the temperature field distributions before cooling and after cooling are obtained. The results show that the temperature drop of winding is 32%, the temperature drop of stator core is 30%, the temperature drop of permanent magnet is 26%, and the temperature drop of rotor is 25%. The spiral channel structure adopted in this paper is reasonable and feasible, which provides a certain theoretical reference value for the research and development of in-wheel motor heat dissipation system.

INDEX TERMS Electric vehicle, in-wheel motor, loss calculation, fluid field, water cooling.

I. INTRODUCTION

Facing the severe challenge of global energy crisis and environmental change, electric vehicle has become a hot spot [1] of automobile industry development in many countries in the world in recent years. As the core component of electric vehicle, the performance of in-wheel is very important and directly affects the comprehensive performance of electric vehicle driven by in-wheel motor. Electric vehicles driven by in-wheel motors usually use high-power permanent magnet motors, which are installed in enclosed narrow space. The large amount of heat generated cannot be released in time. Excessive temperature will lead to demagnetization of in-wheel motor, reduce their reliability and safety, and even affect the performance of the whole vehicle [2]. Therefore, it is very necessary to calculate the heat loss, analyze the temperature field of in-wheel motor, and conduct cooling analysis.

Liu [3] of Dalian University of Technology took an 8.5 kW in-wheel motor prototype as an object, established the finite element simulation model of temperature field of permanent magnet synchronous motor by ThemiNet software, calculated the temperature field distribution under no-load and rated load, and obtained the temperature field distribution of each component. In 2010, Li *et al.* [4] of Hanyang University of Korea developed a permanent magnet synchronous motor (PMSM) for electric vehicles. The air cooling is used as cooling mode in in-wheel motor and the heat dissipation bar was designed on the motor shell to improve the heat dissipation capacity of the in-wheel motor. In 2013, Tianjin Qingyuan

The associate editor coordinating the review of this manuscript and approving it for publication was Rui Xiong.

Electric Vehicle Company Ltd. [5] developed an in-wheel motor with air-cooled heat dissipation. The in-wheel motor uses the high-speed operation of the motor to drive the flow of surrounding air to cool the motor. At the same time, an arc radiator is installed on the end cover of the motor to increase the heat dissipation area of the motor. It improves the heat dissipation capacity of the motor. Li [6] of Athens Polytechnic University analyzed and studied a 4-pole/6-slot permanent magnet in-wheel motor. The in-wheel motor was cooled by liquid, and an oil-cooled channel was designed on the motor shell. The experimental results showed that the cooling effect was better. In 2014, Lee *et al.* [7] in Korea designed and developed an in-wheel motor with oil-cooled cooling method. The cooling method of the motor is to inject cooling oil into the shaft of the motor. Under the pressure of the oil pump, the cooling fluid is circulated and the motor is cooled. Experiment shows that this method has better heat dissipation effect. Yu [8] of General Motors Canada designed an axial flux permanent magnet in-wheel motor. The permanent magnet in-wheel motor uses liquid cooling to cool motor, and its cooling system uses high performance epoxy resin as coolant. The temperature field simulation results show that the cooling of winding and stator is obvious and the cooling effect is excellent. Laskaris and Kladas [9] took a high-speed permanent magnet motor as the research object. Using the coupling method, the temperature distribution in the solid domain of permanent magnet motor was analyzed. The results show that the simulation results are more accurate. Lim and Kim [10] and Xueyan Han of Chongqing University took a high power density permanent magnet synchronous motor as the research object, and established the 3D physical model of the in-wheel motor. Based on the basic theory of fluid mechanics, the coolant of cooling water channel and internal air of the in-wheel motor were simulated and analyzed by CFD software, and the experiments were carried out. The validity of the analysis method is verified by experiments. In 2016, Hsu *et al.* [11] and Gaopeng of Tianjin University proposed the oil cooling mode of in-wheel motor based on the finite element method of 3D temperature field. According to the structure of outer rotor in-wheel motor, the model of in-wheel motor with oil cooling mode was established, and the temperature field of each component of in-wheel motor under different cooling modes was calculated and obtained.

In this paper, the 10KW outer rotor in-wheel motor is taken as the research object. Firstly, the finite element model of electromagnetic field of in-wheel motor is established by Ansoft Maxwell software. Then, the thermal losses are simulated and calculated respectively. Finally, the calculated losses are used as heat sources and are imported into Ansys Workbench for the coupling analysis of electromagnetic field and temperature field.

II. LOSS ANALYSIS OF IN-WHEEL MOTOR

Based on the 10KW in-wheel motor of an electric vehicle, the motor is modeled and simulated by Maxwell software. Firstly, according to the actual demand of in-wheel motor, the main technical parameters of the motor are optimized [15]. The list of basic parameters of in-wheel motor is shown in Table 1. Two-dimensional electromagnetic field model is established by Maxwell software. Maxwell 2D model of in-wheel motor is shown in Fig. 1.

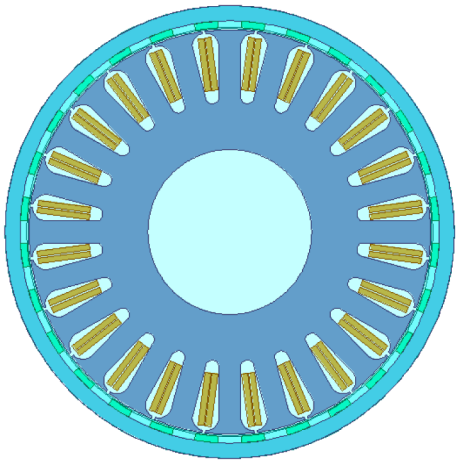

FIGURE 1. Maxwell 2D model of in-wheel motor.

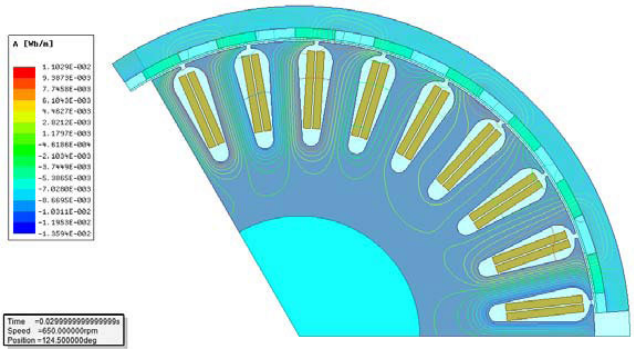

FIGURE 2. Distribution of magnetic line of force at the time of 0.029s.

The transient load field of in-wheel motor is simulated by Maxwell software. The distribution of magnetic line of force and magnetic flux density at the time of 0.029s under rated load state of in-wheel motor are obtained, which are shown in Fig.2 and Fig.3. Fig.2 shows that the maximum magnetic line of force is at the end of stator slot near air-gap, which is mainly caused by the interaction between stator winding current and permanent magnet magnetic field. Fig.3 shows that the magnetic flux density between permanent magnet and stator slot is also large, but the magnetic flux density between different stator slots is roughly equal. The magnetic flux density in the outer rotor is more uniform, and the difference is not significant. In the in-wheel motor, the magnetic flux density in the stator center is the smallest, and the closer along the motor center, the smaller the magnetic flux density.

It can be seen from the above that the distribution of magnetic line of force and magnetic flux density of the in-wheel motor are in line with the design theory, so the correctness of the model is verified and further research can be conducted.

TABLE 1. List of basic parameters of in-wheel motor.

parameter	value	parameter	value
rated power (KW)	10	stator outer diameter (mm)	306
rated voltage (V)	300	rotor outer diameter (mm)	343
rated speed (r/min)	650	effective length (mm)	48
rated torque (Nm)	150	air-gap length (mm)	0.8
rated current (A)	33.3	number of pole-pair	12
frequency (HZ)	130	number of slot	27

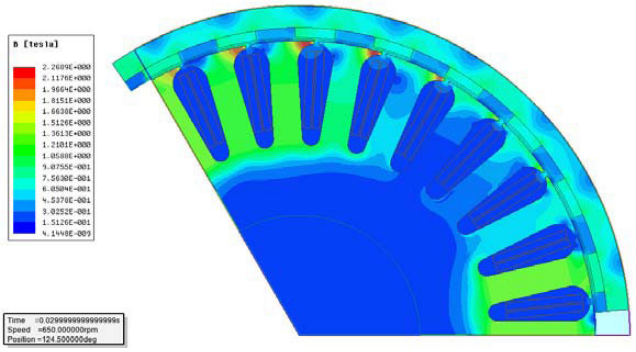

FIGURE 3. Distribution of magnetic flux density at the time of 0.029s.

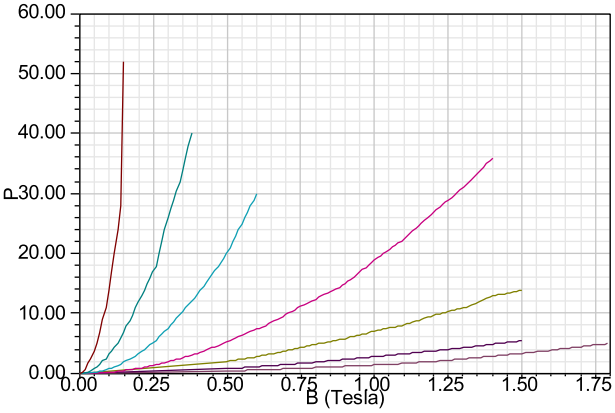

FIGURE 4. Core loss of DW310-35 at multi-frequency (BP curve).

The total losses of in-wheel motor mainly include core loss, copper loss, eddy current loss and mechanical loss. Most of the heat loss of the motor is converted into heat, which is transmitted in the motor. Then, the existing heat changes the distribution of temperature field in the motor. The total losses of in-wheel motor can be expressed as [14], [16]:

$$P_z = P_{Cu} + P_{Fe} + P_{me} + P_{mf} \tag{1}$$

$$P_{Fe} = P_h + P_e + P_{ex} = C_h f B_m^n + C_e f^2 B_m^2 + C_{ex} f^{1.5} B_m^{1.5} \tag{2}$$

$$P_{cu} = mI^2R \tag{3}$$

$$P_{me} = \frac{L_a V k_{me}^2 f_{me}^2 B_{me}^2 L_b^2}{12\rho_1 (L_a + L_b)} \tag{4}$$

Here: P_{Cu} is copper loss of winding;
P_{Fe} is core loss;
P_{me} is eddy current loss of permanent magnet;
P_{mf} is mechanical loss;
C_h is hysteresis loss coefficient;
C_e is eddy current loss coefficient;
m is phase number of in-wheel motor;
I is effective value of phase current of one cycle;
R is resistance value of motor at this temperature;
L_a is axial length of permanent magnet;
f_{me} is alternate frequency of magnetic field;
ρ_1 is resistivity of permanent magnet;
B_{me} is maximum magnetic flux density of permanent magnet.

For the permanent magnet synchronous in-wheel motor, the material of stator and rotor is made of non-oriented silicon steel sheet DW310-35. The data of BP curve and BH curve have been found and fitted. The core loss curve (BP curve) and magnetization curve (BH curve) are shown in Fig.4 and Fig.5 respectively.

The innovation is that the iron loss curve at single frequency is only used in previous studies on iron core loss, so the loss value calculated by simulation is not accurate enough to intuitively reflect the temperature rise of in-wheel motors. The multi-frequency iron loss curve is adopted in this paper, which is helpful to improve the simulation accuracy and the calculation result is more accurate.

Using Ansoft Maxwell software, the internal losses of the motor are analyzed by finite element method. The losses of the permanent magnet in-wheel motor under the speed of 650r/min at rated load are shown in Table 2. The losses of the permanent magnet in-wheel motor under the speed of 650r/min at the load of 1.1 times are shown in Table 3.

Table 2 and table 3 shows: in-wheel motor in the rated speed under different load working state of the loss of value is different. In the load state of 1.1 times is much higher than the loss value of the rated load, Therefore, in the cooling study in the following paper, the imported loss value is the load loss value of 1.1 times. If the cooling effect can reach the expected temperature under extreme conditions, the cooling effect under rated load will not be a problem.

TABLE 2. Losses of the permanent magnet in-wheel motor under the speed Of 650r/min at rated load.

copper loss	core loss	eddy current loss	air friction loss
730W	100W	104mW	30W

TABLE 3. Losses of the permanent magnet in-wheel motor under the speed of 650r/min at rated load of 1.1 times.

copper loss	core loss	eddy current loss	air friction loss
780W	112W	120mW	30W

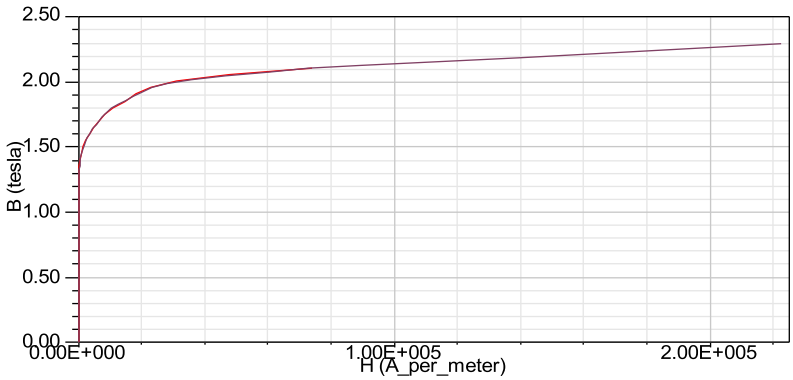

FIGURE 5. Magnetization curve of DW310-35 (BH curve).

III. ESTABLISHMENT OF TEMPERATURE FIELD MODEL

A. THE EQUIVALENCE OF WINDING

When the equivalent thermal model of stator winding is established, the whole winding can be treated as an equivalent part, and the equivalent thermal conductivity coefficient of the winding must be calculated. Therefore, the corresponding assumptions should be made [17]: (1) The conductors in the slot are uniformly arranged, and the temperature difference is neglected; (2) The insulating paint of copper wire is uniformly distributed; (3) The temperature changes in the insulating layer and the filling paint of copper wire are linear; (4) The impregnating paint of the winding is fully filled. Therefore, the stator slot insulation includes copper wire varnish impregnating paint insulation and slot insulation, and its equivalent thermal conductivity coefficient is as follows:

$$\varepsilon = \sum_{i=1}^{n} \delta_i / \sum_{i=1}^{n} \delta_i / \alpha_i \tag{5}$$

Here: ε is the equivalent thermal conductivity coefficient of the insulating layer in the stator slot;

α_i is the thermal conductivity coefficient of the insulating materials in the stator slot;

δ_i is the thickness of the insulating layer in the stator slot.

B. CALCULATION OF HEAT EXCHANGE COEFFICIENT

Accurate calculation of heat dissipation coefficient of each component of in-wheel motor is very important to the simulation analysis and calculation of motor temperature field. The calculation of surface heat dissipation coefficient is relatively complex, and empirical formula is usually used to calculate it.

(1) Heat dissipation coefficient of stator core end face [18]

$$\alpha_s = \frac{1 + 0.04v}{0.045} \tag{6}$$

Here: v is the outer diameter linear velocity of the rotor of in-wheel motor.

(2) Heat dissipation coefficient of in-wheel motor shell surface

$$\alpha_m = 14\left(1 + 0.5\sqrt{v}\right)^3 \sqrt{\frac{T_0}{25}} \tag{7}$$

Here: T_0 is the air temperature of the outer wall of the machine base.

(3) Heat dissipation coefficient of rotor end face of in-wheel motor

$$\alpha_\gamma = 28\left(1 + \sqrt{0.45v}\right) \tag{8}$$

Here: v is the inner wall temperature of the machine base.

(4) Heat dissipation coefficient of clearance between stator and rotor of in-wheel motor

When calculating the temperature field of in-wheel motor, the air between stator and rotor is in a flow state. In this paper, the air-gap is treated equivalently [19].

The mathematical expression of Reynolds number in air-gap of outer rotor in-wheel motor can be expressed

as follows:

$$\mathrm{Re} = \frac{\omega_{\varphi_1}\delta}{\tau} \tag{9}$$

$$\mathrm{Re}_{cr} = 41.2\sqrt{\frac{D_{i2}}{\delta}} \tag{10}$$

When $\mathrm{Re} < \mathrm{Re}_{cr}$, the air flow of air gap can be judged as laminar flow, and the equivalent thermal conductivity coefficient of air-gap is approximately equal to the thermal conductivity coefficient of air; when $\mathrm{Re} > \mathrm{Re}_{cr}$, the air flow of air-gap can be judged as turbulent flow. At this time, the calculation equation of the equivalent thermal conductivity coefficient of air gap between stator and rotor is as follows:

$$\lambda_{eq} = 0.0019\eta^{-2.9084}\mathrm{Re}^{0.4614\ln(3.33361\eta)} \tag{11}$$

Here: $\eta = \mathrm{D}_1/\mathrm{D}_{i2}$;
ω_{φ_1} is the circumferential speed of the rotor;
δ is the length of the air-gap of the motor;
τ is the air kinematic viscosity coefficient.

IV. ESTABLISHMENT AND SIMULATION OF WATER COOLING MODEL

A. ESTABLISHMENT OF WATER COOLING MODEL

The cooling channel design of in-wheel motor should meet the following design requirements:

(1) The contact surface between the fluid and the in-wheel motor in the waterway should be as large as possible.

(2) The channel should be designed as smoothly as possible to reduce the resistance of the fluid in the flow process.

(3) The surface heat transfer coefficient of cooling water channel should be as large as possible to improve its heat dissipation capacity.

(4) Coolant with relatively large thermal conductivity should be used as cooling medium as far as possible.

(5) Cooling water pipes should be safe, stable and cheap to maintain.

The control model suitable for the water-cooling model of in-wheel motor in this paper is $k-\varepsilon$ turbulence model [20], and its mathematical expression is as follows (12) and (13), as shown at the bottom of this page.

Here: G_k is the turbulent energy generation term caused by average velocity gradient;

G_b is the turbulent energy generation term caused by buoyancy;

Y_m is the contribution of pulsation expansion in compressible turbulence;

S_k&S_ε are the original term of definition;

$G_{1\varepsilon}$&$G_{2\varepsilon}$&$G_{3\varepsilon}$ are the empirical coefficient.

FIGURE 6. 3D model of the cooling channel.

According to the actual demand of this paper, the circumferential helical cooling structure is chosen as the cooling channel structure of in-wheel motor. In addition, the cooling pipe inlet and outlet are placed on different sides of the motor. The water-cooling channel model is established, and the simple equivalent treatment is carried out. The cooling channel is installed on the frame inside the stator, and the 3D model of the cooling channel is shown in Fig. 6.

B. CALCULATION OF COOLANT FLOW VELOCITY AND INLET-OUTLET PRESSURE DIFFERENCE

In this paper, the motor is an outer rotor in-wheel motor. When the in-wheel motor works stably, the heat generation and heat dissipation of the motor itself have reached a heat balance state. The water cooling system in this paper is the main heat dissipation system of the motor. If all the heat generated by the in-wheel motor is taken away by the cooling system, when the temperature difference between the inlet and outlet is T, the flow rate and the velocity of the cooling system can be calculated by empirical formula [21], [22]. The formula is as follows.

$$P_{loss} = u \times \rho\frac{\pi d^2}{4} \times c_p \times (T_{out} - T_{in}) \times 10^{-6} \tag{14}$$

Here: P_{loss} is the total loss of in-wheel motor;
T_{out} is the inlet temperature of cooling water jacket;
T_{in} is the outlet temperature of cooling water jacket;
c_p is the specific heat capacity of water;
ρ is the density of fluid;
u is the flow rate of fluid;
m is the flow rate of fluid.

According to the above formula, the velocity of coolant fluid in the cooling channel is approximately 3.0 m/s.

For in-wheel motor of electric vehicle, the water resistance of cooling water channel is one of the important factors to measure whether the design of cooling water channel is reasonable or not. Generally speaking, the distance flowing through the fluid and the cross-sectional area of the water channel are the main factors affecting the resistance along the

$$\frac{\partial(\rho k)}{\partial t} + \frac{\partial(\rho k u_i)}{\partial x_i} = \frac{\partial}{\partial x_j}\left[\left(\mu + \frac{\mu_i}{\alpha_k}\right)\frac{\partial k}{\partial x_j}\right] + G_k + G_b - \rho\varepsilon - Y_m + S_k \tag{12}$$

$$\frac{\partial(\rho\varepsilon)}{\partial t} + \frac{\partial(\rho\varepsilon u_i)}{\partial x_i} = \frac{\partial}{\partial x_j}\left[\left(\mu + \frac{\mu_i}{\alpha_\varepsilon}\right)\frac{\partial \varepsilon}{\partial x_j}\right] + G_{1\varepsilon}\frac{\varepsilon}{k}(G_k + G_{3\varepsilon}G_b) - G_{2\varepsilon}\rho\frac{\varepsilon^2}{k} + S_\varepsilon \tag{13}$$

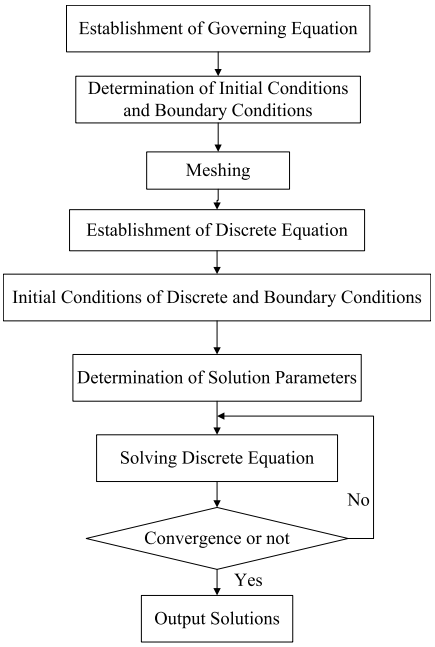

FIGURE 7. Solution flow chart of CFD.

path, and the correlation formula is as follows [23].

$$h_f = \lambda_f \frac{v^2}{d_e} \frac{L_{all}}{2g} \tag{15}$$

Here: h_f is the resistance along the path;
L_{all} is the total length of channel;
λ_f is the resistance coefficient;
d_e is the hydraulic diameter of the channel;
v is the flow rate of cooling fluid;
g is the acceleration of gravity.

C. FLOW FIELD SIMULATION ANALYSIS OF COOLING SYSTEM

Firstly, in order to simulate and analyze the fluid characteristics of the cooling medium in the cooling channel of in-wheel motor, based on the basic theory of hydrodynamics, the governing equation is established and the turbulence model is determined. Secondly, a three-dimensional solution model is established, the model is meshed, and the boundary conditions, initial conditions and control parameters are determined. Finally, the calculation results are post-processed, and the related nephograms are obtained by iteration. The solution flow chart of CFD is shown in Fig. 7.

Secondly, mesh generation of in-wheel motor geometric model is carried out, and the mesh generation diagram of cooling channel shown in Fig. 8 below is obtained. In order to obtain more accurate partial nephogram of temperature field, it is necessary to mesh accurately. At the same time, considering the efficiency of computer simulation calculation, the mesh generation of motor is also not to be too small. In this paper, the mesh number of cooling channel is 30120.

Then, the boundary conditions and necessary settings of the helical channel model are set. According to the calculated

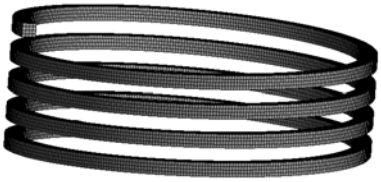

FIGURE 8. Mesh generation diagram of cooling channel.

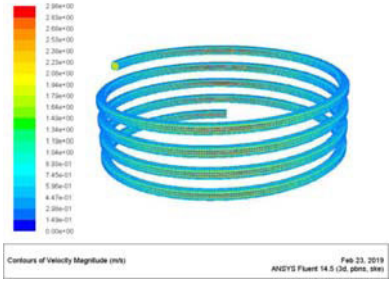

FIGURE 9. Velocity nephogram of the cooling medium.

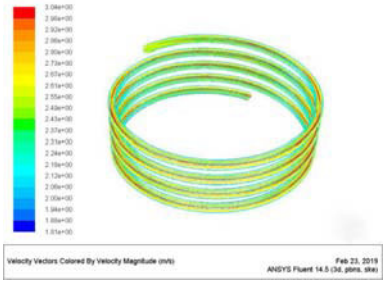

FIGURE 10. Velocity vector nephogram of the cooling medium.

inlet velocity of cooling medium, the inlet velocity is set to 3.0m/s, the number of iterations is set to 600, and the relative error is set to 0.01%. The velocity nephogram of the cooling medium is shown in Fig. 9. The velocity vector nephogram of the cooling medium is shown in Fig. 10. Fig. 9 shows that when the inlet flow velocity is 3.0m/s, the cooling medium flow velocity of the helical channel fluctuates between 0.5m/s and 2.3m/s. The flow velocity of the fluid in the channel is relatively uniform on the whole, and the water paths of each layer are similar. The results indicate that the resistance of the coolant in the channel is not very different. Because of there is no major change of angle in helical channel, the channel is smooth and the cooling effect is better.

Fig. 10 shows that when the inlet flow velocity is 3.0m/s, the velocity vector of the cooling medium in the pipe fluctuates between 2.1m/s and 2.8m/s. The velocity vector of the fluid in the channel is relatively uniform on the whole, mainly because the number of bends in the cooling channel is less and the water resistance is smaller.

V. TEMPERATURE FIELD ANALYSIS OF IN-WHEEL MOTOR WITH WATER COOLING SYSTEM

Before simulating the temperature field of in-wheel motor with cooling channel, it is necessary to calculate the thermal

TABLE 4. Comparison of the temperature changes of in-wheel motor before cooling and after cooling.

components	Maximum temperature after cooling	Maximum temperature before cooling	Temperature different	Proportion
Winding (°C)	123.26	182.4	59.14	32%
Stator core (°C)	90.895	130.34	39.445	30%
Permanent magnet (°C)	62.864	85.537	22.673	26%
Rotor (°C)	59.705	80.477	20.477	25%

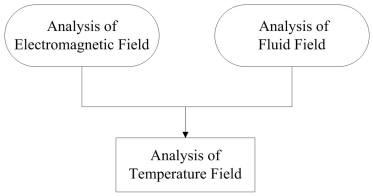

FIGURE 11. Coupling principle.

losses of the main components of the motor under overload condition. At the same time, CFD software is used to simulate and analyze the fluid field of the coolant in the cooling water channel, and the heat dissipation coefficient curve is calculated. Finally, the simulation results obtained by the above simulation software are imported into the thermal analysis module of Ansys Workbench transient field, and the temperature distribution nephogram of the main components of the motor is obtained. The coupling principle is shown in Fig. 11.

In this paper, the temperature field coupling simulation of in-wheel motor with water cooling system is carried out. In order to get the temperature distribution nephogram of components in in-wheel motor under overload condition, the ambient temperature is set to 22 °C, and the material parameters and boundary conditions are set. Considering the configuration of the computer and the efficiency of simulation, the simulation step is set to 0.5s and the total simulation time is set to 600 s. The temperature field simulation starts from 0 s, and the iteration calculation is carried out continuously until the final simulation calculation is completed. The diagram of the coupling of electromagnetic field, fluid field and temperature field is shown in Fig. 12.

As shown in Fig. 13, the stator temperature distribution nephogram shows that the cooling water channel of in-wheel motor has a great influence on the stator temperature field heat dissipation under overload condition. Fig. 13 (b) shows that the maximum temperature of the motor stator is about 130 °C before water cooling. Fig. 13 (a) shows that the maximum temperature of the motor stator is about 91 °C after water cooling. The highest temperature of the stator appears in the stator yoke. This is mainly because the smaller heat dissipation area of the stator yoke and the slower heat dissipation efficiency, and the better heat dissipation condition of the stator tooth.

As shown in Fig. 14, the winding temperature distribution nephogram shows that the water cooling system of in-wheel

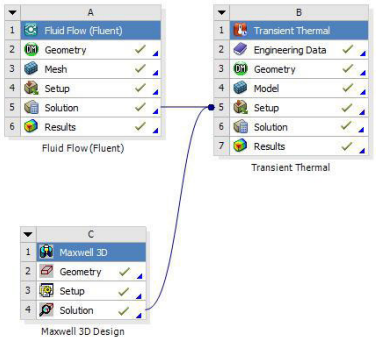

FIGURE 12. Diagram of the coupling of electromagnetic field, fluid field and temperature field.

motor has a great influence on improving the heat dissipation ability of the motor. Fig. 14 (b) shows that the maximum temperature of the winding is about 182 °C before water cooling. Fig. 14 (a) shows that the maximum temperature of the winding is about 123 °C after water cooling. The temperature of the winding in the upper surface area is higher than that in the lower surface area, and the temperature distribution has certain regularity. This is mainly because the current input in the winding is three-phase alternating current. At any moment, the current value in the winding is different, so it presents the situation of high temperature in some areas and low temperature in some areas.

As shown in Fig. 15, the maximum temperature of the rotor before water cooling is about 80 °C, and the highest temperature of the rotor after water cooling is about 60 °C. The minimum temperature of the rotor appears in the outermost layer, which is mainly the outer rotor motor is used in this paper, so the outermost layer of the rotor has better heat dissipation efficiency. The highest temperature region of the rotor mainly appears in the inner layer of the rotor, which is mainly close to the winding and permanent magnet, and is greatly affected by their temperature.

As shown in Fig. 16, the maximum temperature of the permanent magnet before water cooling is about 137 °C, and after cooling is about 72.4 °C, which is reduced by about 23 °C.

From the above analysis, before water cooling and after water cooling, the temperature of the main components of the motor has been significantly reduced. Table 4 is the comparison of the temperature changes of in-wheel motor before and after cooling. Table 4 shows

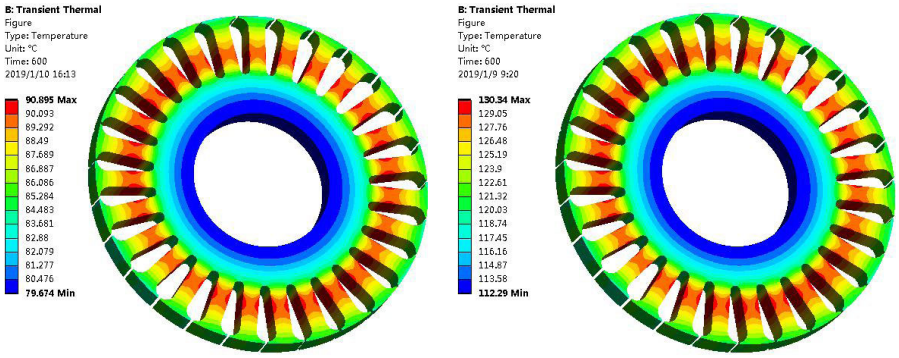

(a) After water cooling (b) Before water cooling

FIGURE 13. Stator temperature distribution nephogram.

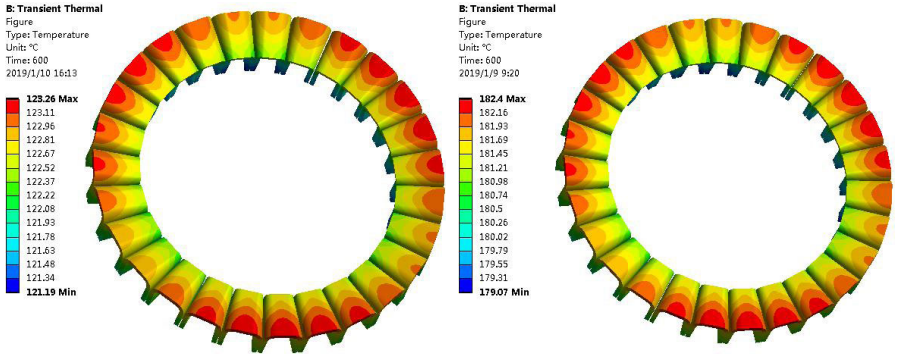

(a) After water cooling (b) Before water cooling

FIGURE 14. Winding temperature distribution nephogram.

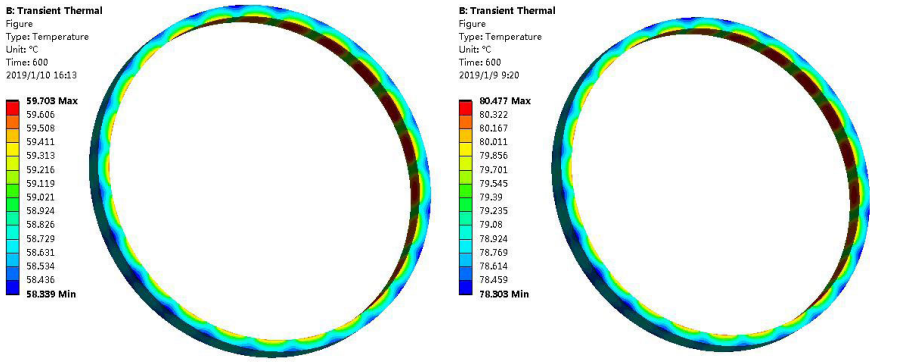

(a) After water cooling (b) Before water cooling

FIGURE 15. Rotor temperature distribution nephogra.

that the water cooling heat dissipation system has a greater impact on improving the heat dissipation capacity of the motor, which shows the rationality of the water cooling structure.

VI. DISCUSSION

This paper takes an in-wheel motor as the research object, carries out a series of research work, and obtains relevant conclusions. However, due to limited personal ability, time

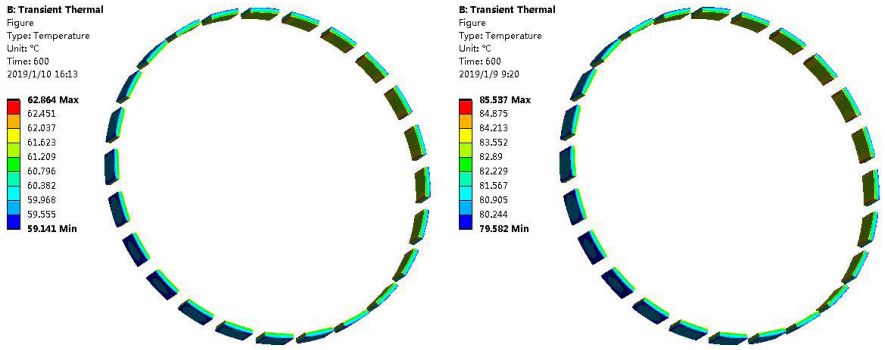

(a) After water cooling (b) Before water cooling

FIGURE 16. Permanent magnet temperature distribution nephogram.

and energy, the paper still needs to be further improved in many aspects:

(1) In this paper, the coupling analysis of electromagnetic field, temperature field and fluent field of the electric car in-wheel motor is carried out. However, it is studied the theoretical level, and the real vehicle test is lacked. With the existing conditions and the limitation of funding, it is difficult to meet the related test conditions, only do the relevant theoretical analysis and simulation calculation and analysis, Therefore, it is necessary to improve real vehicle tests.

(2) In the coupling simulation calculation of electromagnetic field and temperature field of in-wheel motors, the influence of performance of various materials of the motor with the temperature change are not considered, but only carried out unidirectional coupling, and its simulation accuracy needs to be further improved. Therefore, the follow-up research should conduct bidirectional coupling simulation of in-wheel motor.

VII. CONCLUSION

(1) The inlet flow velocity is set to 3.0m/s, and the cooling medium flow velocity of the helical structure channel fluctuates between 0.5m/s and 2.3m/s. The flow velocity of the fluid in the channel is relatively uniform on the whole, and the water paths of each layer are similar, indicating that the resistance of the coolant in the channel is not very different,

(2) When the inlet flow velocity is 3.0m/s, the velocity vector of the cooling medium in the pipe fluctuates between 2.1m/s and 2.8m/s, and the velocity vector of the fluid in the water channel is relatively uniform on the whole.

(3) The cooling channel of in-wheel motor has great influence on the stator temperature field heat dissipation. Before water cooling, the maximum temperature of the motor stator is about 130 C, and after water cooling, the maximum temperature of the motor stator is about 91 C. The temperature drop of stator is about 30%. The maximum temperature of stator appears in the stator yoke area.

ACKNOWLEDGMENT

The authors would like to thank anonymous reviewers for their helpful comments and suggestions to improve the manuscript.

REFERENCES

[1] G. Ma, "Trends and policy orientation analysis of new energy power technologies," *Internal Combustion Engines Accessories*, vol. 278, no. 2, pp. 183–185, 2019.

[2] S. Lu, X. Xu, L. Chen, F. Wang, and W. Wang, "Coordinated control of electronic differential speed and differential power steering for vehicles driven by in-wheel motors," *J. Mech. Eng.*, vol. 53, no. 16, pp. 78–85, 2017.

[3] Z. Liu, "Power matching of in-wheel motor drive system and fuel cell electric vehicle," Ph.D. dissertation, Jilin Univ., Changchun, China, 2015.

[4] M. Li, K. Yang, J. Wang, Z. Tian, and P. Li, "Research on ABS control logic for hub-driven electric vehicles," *Automotive Technol.*, vol. 7, pp. 42–47, Mar. 2019.

[5] H. Yao, "Temperature rise and cooling characteristic simulation of electric vehicle in-wheel motor," Ph.D. dissertation, Jilin Univ., Changchun, China, 2018.

[6] X. Li, "Design and magneto-thermal coupling analysis of high power density permanent magnet synchronous motor," Ph.D. dissertation, Dalian Univ. Technol., Dalian, China, 2016.

[7] B. H. Lee, S.-I. Kim, J.-J. Lee, J.-P. Hong, and C.-S. Park, "Design of an interior permanent magnet synchronous in-wheel for electric vehicles," in *Proc. Int. Conf. Elect. Mach. Syst. (ICEMS)*, Incheon, South Korea, Oct. 2010, pp. 1226–1229.

[8] F. Yu, "An air-cooled heat dissipation mechanism for electric vehicle in-wheel motor," U.S. Patent 10 371 582 9A, People's Republic of China, 2013.

[9] K. I. Laskaris and A. G. Kladas, "Liquid cooled permanent-magnet traction motor design considering temporary overloading," in *Proc. 20th Int. Conf. Elect. Mach. (ICEM)*, Marseille, France, Sep. 2012, pp. 2677–2682.

[10] D. H. Lim and S. C. Kim, "Thermal performance of oil spray cooling system for in-wheel motor in electric vehicles," *Appl. Thermal Eng.*, vol. 63, no. 2, pp. 577–587, 2014.

[11] J. S. Hsu, T. A. Burress, S. T. Lee, R. H. Wiles, C. L. Coomer, J. W. McKeever, and D. J. Adams, "16,000-RPM interior permanent magnet reluctance machine with brushless field excitation," in *Proc. IEEE Ind. Appl. Soc. Annu. Meeting*, Oct. 2008, pp. 1–6.

[12] Z. Kolondzovski, A. Belahcen, and A. Arkkio, "Multiphysics thermal design of a high-speed permanent-magnet machine," *Appl. Therm. Eng.*, vol. 29, pp. 2693–2700, Sep. 2009.

[13] Q. Shen and X. Han, "Fluid field analysis of water-cooled high power density permanent magnet synchronous motor for vehicles," *Micromotor*, vol. 47, no. 12, pp. 1–5, 2014.

[14] X. Wang and P. Gao, "Three-dimensional temperature field analysis of oil-cooled permanent magnet in-wheel motors for electric vehicles," *J. Motor Control*, vol. 20, no. 3, pp. 36–42, 2016.
[15] Q. Chen, H. Shu, S. Zhuang, K. Ren, and J. Fu, "Magneto-thermal coupling analysis on the in-wheel motors of micro electric vehicles," *Automot. Eng.*, vol. 35, no. 7, pp. 593–598, 2013.
[16] Y. Huang, Q. Hu, and J. Zhu, "Three-dimensional magneto-thermal coupling analysis of high-speed claw-pole motor considering rotating iron consumption," *J. Electr. Technol.*, vol. 5, pp. 54–60, Jun. 2010.
[17] Y. Shao and Z. Liu, "Global three-dimensional transient temperature field analysis of induction motors," *China J. Electr. Eng.*, vol. 30, no. 30, pp. 114–120, 2010.
[18] X. Wei, "Temperature field analysis and cooling system research of permanent magnet synchronous motor," Ph.D. dissertation, Xiangtan Univ., Xiangtan, China, 2017.
[19] V. Hatziathanassiou, J. Xypteras, and G. Archontoulakis, "Electrical-thermal coupled calculation of an asynchronous machine," *Archiv für Elektrotechnik*, vol. 77, no. 2, pp. 117–122, 1994.
[20] F. Wang, *Computational Fluid Dynamics Analysis*. Beijing, China: Tsinghua Univ. Press, 2004.
[21] X. Wang and J. Du, "Application of CFD fluid-solid coupling thermal analysis to water cooling system of high power density motor for vehicles," *J. Electr. Technol.*, vol. 30, no. 9, pp. 30–38, 2015.
[22] Y. Wei, D. Meng, and J. Wen, *Heat Exchange in Motor*, 1st Ed. Beijing, China: Machinery Industry Press, 1998.
[23] X. Yang and X. Zhang, "Design of Z-shaped cooling water channel for motor shell," *Motor Control Appl.*, vol. 43, no. 9, pp. 62–65, 2016.

QIPING CHEN received the Ph.D. degree in mechanical engineering from Chongqing University, Chongqing, China, in 2013. He is currently an Associate Professor with the School of Mechatronics and Vehicle Engineering, East China Jiaotong University, China. His research interests include electric vehicles, hybrid vehicles, and mechatronics.

HAO SHAO received the master's degree from East China Jiaotong University. His research interest includes electromagnetic thermal analysis of electric vehicle in-wheel motor.

JUANLIN HUANG received the master's degree from East China Jiaotong University. His research interest includes electromagnetic thermal analysis of electric vehicle in-wheel motor.

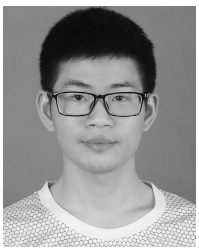

HAOYU SUN received the master's degree from East China Jiaotong University. His research interest includes electric vehicle electro-hydraulic braking technology.

JIACHAO XIE received the master's degree from East China Jiaotong University. His research interest includes unmanned driving technology.